

Phys. Rev. **185**, 548 (1969).

²F. S. Ham, Phys. Rev. **160**, 328 (1967).

³J. Chappert, R. B. Frankel, A. Missetich, and N. A. Blum, Phys. Rev. **179**, 578 (1969).

⁴H. R. Leider and D. N. Pipkorn, Phys. Rev. **165**, 494 (1968).

⁵J. Chappert, R. B. Frankel, A. Missetich, and N. A. Blum, J. Phys. Suppl. C **1**, 941 (1971).

⁶J. Y. Wong, Phys. Rev. **168**, 337 (1968).

⁷R. L. Hartman, E. L. Wilkinson, and J. G. Castle, Bull. Am. Phys. Soc. **12**, 642 (1967).

⁸H. M. Rosenberg and J. K. Wigmore, Phys. Letters **24A**, 317 (1967).

⁹J. K. Wigmore, H. M. Rosenberg, and D. K. Garrod, J. Appl. Phys. **39**, 682 (1968).

¹⁰R. E. Watson and A. J. Freeman, Phys. Rev. **123**, 2027 (1961).

¹¹R. Ingalls, Phys. Rev. **188**, 1045 (1969).

¹²Y. Hazony, Phys. Rev. B **3**, 711 (1971).

¹³D. P. Johnson and R. Ingalls, Phys. Rev. B **1**, 1013 (1970).

¹⁴C. E. Johnson, Proc. Phys. Soc. (London) **92**, 748 (1967).

¹⁵J. Chappert, J. R. Regnard, and J. Danon, Compt. Rend. **272**, 1070 (1971).

Temperature Dependence of the Spin-Lattice Interaction for Gd^{3+} in ThO_2 and CeO_2 †

S. B. Oseroff and R. Calvo*

*Centro Atómico Bariloche, Comisión Nacional de Energía Atómica,
Instituto de Física "Dr. José A. Balseiro," Universidad Nacional de Cuyo,
San Carlos de Bariloche, Argentina*

(Received 21 July 1971)

The second- and fourth-order spin-lattice coefficients of Gd^{3+} in cubic positions of ThO_2 and CeO_2 crystals have been measured as a function of temperature between 4 and 360 °K by electron-paramagnetic-resonance experiments in uniaxially stressed crystals. The second-order coefficients are considerably different for the two crystals, and these coefficients show a large variation with temperature. A detailed theoretical calculation of these coefficients has not been carried out; however, it is possible to qualitatively interpret the observed temperature variation in terms of effects due to the modulation of the orbit-lattice interaction by the lattice vibrations. The temperature-variation curves are explained using an Einstein model for the vibrations of the oxygen ligands of the paramagnetic ions. The fourth-order coefficients are similar for the two crystals and are temperature independent in the range studied. The effect of a hydrostatic strain on the energy levels of the ion is used to explain the observed temperature variation of the cubic field parameter in terms of the thermal expansion of the crystal.

I. INTRODUCTION

The interpretation of the crystal-field splittings of ions with a half-filled shell of electrons, Cr^{3+} , Mn^{2+} , and Fe^{3+} of the 3d group and Eu^{2+} , Gd^{3+} , and Tb^{3+} of the rare-earth group, has involved serious difficulties. The crystalline electric field acting alone cannot remove the degeneracy of the ground level of these S-state ions and it is necessary to consider high-order processes involving spin-dependent interactions together with the crystal-line field. A great deal of experimental information obtained by electron-paramagnetic-resonance (EPR) techniques exists for these ions and many theoretical papers dealing with this problem are found in the literature. The reader is referred to Refs. 1 and 2, where an important part of the theoretical work done on this problem until 1966 is quoted.

Important progress has been made in the understanding of the S-state iron-group ions and, even

though a good fit between theory and experiment does not yet exist, an order of magnitude agreement has been found.² However, less progress has been made in the explanation of the splittings of the ground state of the rare-earth S-state ions, even though experimental data exist for several cubic crystals³ and for many lattices of lower symmetry.

An attempt to estimate the ionic contributions to the ground-state splitting of trivalent gadolinium in lanthanum ethyl sulphate has been made by Wybourne.¹ Wybourne considers the contributions coming from several mechanisms involving the crystal field with other interactions in different orders of perturbation and also relativistic effects, configuration mixing, and nonlinear electrostatically correlated crystal-field interactions. The result of the calculation does not agree with the experimental values and Wybourne suggests that the correct explanation should involve the details of the interaction of the gadolinium ion with the lig-

ands.

It appears to us that additional experimental data, obtained by more sophisticated EPR techniques, where the variation of the splitting of the ionic levels can be measured as a function of some other parameters, could lead to a better understanding of the mechanisms contributing to the splitting. The measurement of the splittings or shifts of the energy levels of the ions when the crystal is deformed by an externally applied stress has proved to be a powerful method for this purpose.⁴ In cubic crystals additional components of the crystalline field with cubic, tetragonal, and trigonal symmetry with variable magnitude are introduced by the strain, and the induced splittings or shifts of the energy levels of the ions can be deduced from the shifts in magnetic field of the EPR lines.

Uniaxial stress experiments involving S-state ions in cubic crystals have been performed by Fehér⁴ for the iron group and by Calvo *et al.*⁵ for the rare earths. The spin-lattice coefficients of the iron-group ions Mn²⁺ and Fe³⁺ in MgO have been calculated by Sharma *et al.*,² who obtained reasonable agreement with the experimental value⁴; they found that the main contribution comes from a process originally proposed by Blume and Orbach⁶ which involves the admixtures to the ground state of excited terms which are mixed by the cubic field via the spin-orbit interaction. Owing to this admixture, it is possible to destroy the degeneracy of the ground level with the electric field induced by the deformation. In a previous work⁷ we calculated the contribution of the Blume-Orbach mechanism to the spin-lattice coefficients of Gd³⁺ in CaF₂. A contribution was found though only for the second-order trigonal coefficient.

In this paper we report data taken with the uniaxial stress method; the spin-lattice coefficients of Gd³⁺ in cubic positions of ThO₂ and CeO₂ crystals have been measured between liquid-helium and room temperatures.⁸ The two second-order spin-lattice coefficients, related to tetragonal and trigonal deformations, and the three fourth-order coefficients, related to hydrostatic, tetragonal, and trigonal deformations, have been measured within this range. The three fourth-order coefficients do not change in this temperature range within the experimental errors and are practically the same for the two crystals. In contrast, the two second-order spin-lattice coefficients show very large changes with temperature and, in the case of Gd³⁺ in CeO₂, the trigonal coefficient changes sign as the temperature is varied. The relative changes in the second-order coefficients are approximately the same for the two crystals.

The temperature dependence of the second-order spin-lattice coefficients can be interpreted qualitatively as produced by a phonon-induced mechanism

("explicit effect"⁹). "Implicit effects,"⁹ due to the changes of the elastic constants with temperature or to the lattice expansion, seem to be unimportant in these cases.

Using our value for the fourth-order spin-lattice coefficient related to hydrostatic deformations for Gd³⁺ in ThO₂ we show that the temperature variation of the cubic field parameter is a consequence of the thermal expansion of the crystal.

II. APPARATUS AND EXPERIMENTAL PROCEDURE

The data were taken with a conventional homodyne spectrometer working at 32 GHz. The stress system, which has been described previously,¹⁰ consists mainly of a TE₀₁₁ cylindrical microwave cavity, where the sample is in the center on a quartz pedestal, with a push-rod coming from the head of the cryostat to allow one to stress the sample against the pedestal by putting weights on the top. The system was designed and built in order to minimize any change in the orientation of the sample when the stress is applied, which is the main cause of error in these measurements.⁵ This was achieved by giving mechanical strength to the stress system and by using a guide to inhibit rotations of the push-rod.

The samples were grown by C. B. Finch of Oak Ridge National Laboratory and have about 0.1 at. % of gadolinium ions, which are mostly at cubic positions replacing the Th⁴⁺ and Ce⁴⁺ ions in the crystals. They were polished to a prismatic shape of about 1×1×1.5 mm³, where the orientation of the prism, a <110> direction, is accurately defined by the intersection of two {111} natural cleavage faces of the sample. The stress was applied along this [110] direction within an estimated error smaller than 1°. The data were taken for the magnetic field perpendicular to the stress, in the (110) plane. The values of the spin-lattice coefficients were obtained from the measurement of the shifts of the seven fine structure lines of the Gd³⁺ cubic spectra as a function of the applied stress for the magnetic field H_0 in the three principal directions [001], [110], and [111]. These directions were accurately defined by looking in the screen of an oscilloscope for the maximum or minimum of the splittings of the spectra as H_0 is rotated in the (110) plane. The shifts for a fourth direction of H_0 were measured in some cases as a verification of the results. The line shifts as a function of the applied stress were measured at each temperature not less than 20 times for each line and about 50 times at room temperature. This was done for the magnetic field along each of the three crystalline directions. The maximum applied stress was 5.88×10^8 dyn/cm² (600 kg/cm²) and, for example, the line shifts for this stress when H_0 was along the [001] axis are between 0.2

and 1.1 G with an uncertainty of 20 mG for the different lines. The shifts in magnetic field were measured with the sweeping device of the Hall probe-controlled magnet, whose linearity and calibration were checked with a proton resonance magnetometer. The temperature at the nonfixed points was measured with a copper resistance with an error smaller than 3 °K. It was verified in each case that the shifts in magnetic field depend linearly upon the applied stress.

III. EXPERIMENTAL RESULTS

The EPR spectra of Gd^{3+} in cubic positions of ThO_2 and CeO_2 crystals have been described in great detail by Abraham and co-workers.^{3,11} Strong signals with very narrow linewidths were observed which made these excellent systems with which to perform precise measurements.

The uniaxial stress data were explained with the spin-lattice Hamiltonian proposed in Ref. 5; in a slightly different notation, we have

$$H_{SL} = \sum_{n, \xi; i, \alpha} G_i^{(n, \xi)} O_{i, \alpha}^{(n, \xi)} \epsilon_{i, \alpha}, \quad (1)$$

where the $\epsilon_{i, \alpha}$ are linear combinations of the strain tensor transforming like the α th component of the i th irreducible representation of the cubic group. The $O_{i, \alpha}^{(n, \xi)}$ are linear combinations of the Stevens's equivalent spin operators¹² transforming accordingly; ξ is included for the cases where there is more than one n th-order operator transforming like $\Gamma_{i, \alpha}$. The $G_i^{(n, \xi)}$ are the n th-order spin-lattice coefficients. Owing to the properties of the strain tensor, a homogeneous strain in the crystal can produce only hydrostatic (Γ_{1g}), tetragonal (Γ_{3g}), and trigonal (Γ_{5g}) deformations around a paramagnetic ion in a cubic position. For Gd^{3+} , $S = \frac{7}{2}$ and n can be 2, 4, and 6; two second-order, three fourth-order, and four sixth-order spin-lattice coefficients contribute to H_{SL} in Eq. (1). However, as was reported previously,⁵ only second- and fourth-order terms in H_{SL} give measurable contributions to the shifts.

When the stress is applied along the [110] direction and considering up to fourth-order terms, H_{SL} can be written as

$$\begin{aligned} H_{SL} = & G_{1g}^{(4)} (O_4^0 + 5 O_4^4) \epsilon_{1g} \\ & + [G_{3g}^{(2)} O_2^0 + G_{3g}^{(4)} (O_4^0 - 7 O_4^4)] \epsilon_{3g, \theta} \\ & + [G_{5g}^{(2)} O_2^2(s) + G_{5g}^{(4)} O_4^2(s)] \epsilon_{5g, \zeta}, \quad (2) \end{aligned}$$

where the O_n^m and its matrix elements are given by Hutchings¹³ and

$$\begin{aligned} \epsilon_{1g} = & \epsilon_{xx} + \epsilon_{yy} + \epsilon_{zz}, \quad \epsilon_{3g, \theta} = \frac{1}{4} (2\epsilon_{zz} - \epsilon_{xx} - \epsilon_{yy}), \\ \epsilon_{5g, \zeta} = & \epsilon_{xy}. \end{aligned}$$

In the experiments we measure the external stress

P rather than the local deformation. It is more realistic, then, to use spin-lattice coefficients related to stress rather than to strain⁴; if s_{11} , s_{12} , and s_{44} are the three elastic constants at the position of the impurity, the spin-lattice coefficients related to stress are defined by⁵

$$\begin{aligned} C_{1g}^{(n)} &= G_{1g}^{(n)} (s_{11} + 2 s_{12}), \\ C_{3g}^{(n)} &= G_{3g}^{(n)} (s_{11} - s_{12}), \\ C_{5g}^{(n)} &= G_{5g}^{(n)} s_{44}. \end{aligned} \quad (3)$$

In this notation the spin-lattice Hamiltonian of Eq. (2) can be written as

$$\begin{aligned} H_{SL} = & C_{1g}^{(4)} P (O_4^0 + 5 O_4^4) - \frac{1}{4} C_{3g}^{(2)} P O_2^0 - \frac{1}{4} C_{3g}^{(4)} P \\ & \times (O_4^0 - 7 O_4^4) + \frac{1}{2} C_{5g}^{(2)} P O_2^2(s) + \frac{1}{2} C_{5g}^{(4)} P O_4^2(s), \end{aligned} \quad (4)$$

and the shifts for H_0 parallel to the three directions [001], $[1\bar{1}0]$, and $[1\bar{1}1]$ are obtained from the formulas in Refs. 5 and 14.

In Figs. 1 and 2 we show the experimental shifts for Gd^{3+} in ThO_2 at 290 °K and $P = -1$ dyn/cm² (P is negative because the crystal is compressed in the experiments) for H_0 parallel to [001] and $[1\bar{1}1]$, respectively, together with the calculated contributions coming from each term of the spin-lattice Hamiltonian. Similar agreement was found for $H_0 \parallel [1\bar{1}0]$. The same measurements were performed for Gd^{3+} in ThO_2 and CeO_2 at different temperatures between 4 and 360 °K. The values obtained for the spin-lattice coefficients in both crystals at room temperature are given in Table I; the second-order

(a) 500	167	333		333	167	500
◀	▶▶		▶▶	▶	▶	▶
(b) 846	508	423		423	508	846
◀	◀◀		▶▶	▶▶	▶▶	▶▶
(c) 366	220	183		183	220	366
◀	◀◀		▶▶	▶▶	▶▶	▶▶
TOTAL 17.12	5.61	2.73		2.73	5.61	17.12
◀	◀◀		▶▶	▶▶	▶▶	▶▶
EXPT. 17.1	5.6	2.7		2.7	5.6	17.1
			1/2 ↔ 3/2	-1/2 ↔ 1/2	-3/2 ↔ -1/2	
			-7/2 ↔ -5/2	3/2 ↔ 5/2	-5/2 ↔ -3/2	5/2 ↔ 7/2

FIG. 1. Shifts of the EPR lines of $ThO_2 : Gd^{3+}$ for $P \parallel [110]$ and $H_0 \parallel [001]$ corresponding to a compression of $P = -1$ dyn/cm² at 290 °K. (a) Second-order tetragonal contribution, (b) fourth-order hydrostatic contribution, (c) fourth-order tetragonal contribution; the total calculated shifts and the measured values are shown in the last two lines. The shifts were calculated with the values of the spin-lattice coefficients given in Table I and are in units of 10^{-14} cm⁻¹/(dyn/cm²).

(a)	19.05	6.35	12.70		12.70	6.35	19.05
		← ←				→ →	←
(b)	5.64	3.38	2.82		2.82	3.38	5.64
	←	← ←				→ →	→
(c)	3.36	2.02	1.68		1.68	2.02	3.36
	←	← ←				→ →	→
TOTAL	10.05	11.75	17.20		17.20	11.75	10.05
		← ←				→ →	←
EXPT.	10.0	11.8	17.2		17.2	11.8	10.0
		-1/2 ↔ -3/2	1/2 ↔ -1/2		3/2 ↔ 1/2		
		7/2 ↔ 5/2-3/2 ↔ -5/2			5/2 ↔ 3/2	-5/2 ↔ -7/2	

FIG. 2. Shifts of the EPR lines of $\text{ThO}_2:\text{Gd}^{3+}$ for $P \parallel [110]$ and $H_0 \parallel [1\bar{1}1]$ corresponding to a compression of $P = -1 \text{ dyn/cm}^2$ at 290°K . (a) Second-order trigonal contribution, (b) fourth-order hydrostatic contribution, (c) fourth-order trigonal contribution; the total calculated shifts and the measured values are shown in the last two lines. The shifts were calculated with the values of the spin-lattice coefficients given in Table I and are in units of $10^{-14} \text{ cm}^{-1}/(\text{dyn/cm}^2)$.

coefficients $C_{3g}^{(2)}$ and $C_{5g}^{(2)}$ in both crystals are given in Figs. 3 and 4 as a function of temperature. The fourth-order coefficients are constant, within the experimental errors, between 4 and 360°K and are given in Table I. The errors indicated in the measurement of the shifts of the lines were obtained from the dispersion of the data; from these values and the system of equations which give the shifts of the lines for different orientations of H_0 as a function of P and the spin-lattice coefficients, we obtained the errors given in Table I and Figs. 3 and 4; any systematic error (orientation of P and H_0 , changes of position of the sample when stressed, errors due to friction of the push-rod which transmit the force P to the sample, etc.) is smaller than those given there.

No change of the gyromagnetic factor g of Gd^{3+} in either crystal was detected in our experiments.

IV. DISCUSSION

It is useful to have the values of the spin-lattice coefficients related to strain $G_i^{(n)}$ defined in Eqs. (3). Since the elastic constants at the position of the impurity are not known, it is necessary to assume that they are not much different than those of

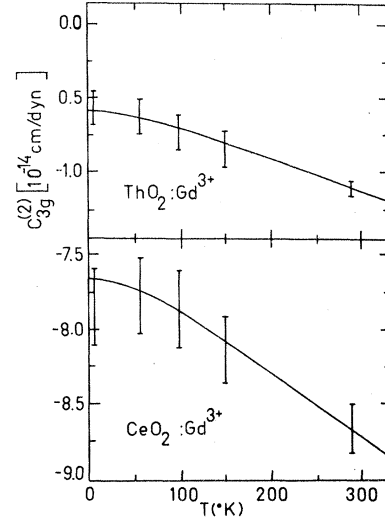


FIG. 3. Temperature dependence of the second-order tetragonal spin-lattice coefficient $C_{3g}^{(2)}$ of Gd^{3+} in ThO_2 and CeO_2 . The solid line is obtained by a least-squares fit of Eq. (6) with the experimental data.

the bulk crystal and we must use these values. The elastic constants of ThO_2 have been measured by Macedo *et al.*¹⁵ at room temperature, but no data seem to exist for CeO_2 ; using these values¹⁵ we calculated the spin-lattice coefficients related to strain for Gd^{3+} in ThO_2 at room temperature. These coefficients are given in Table II.

A. Second-Order Spin-Lattice Coefficients

There is not a general theory which could explain the values of these coefficients; the mechanism proposed by Blume and Orbach⁶ for Mn^{2+} in MgO , which gave some contribution to the trigonal coefficient $G_{5g}^{(2)}$ of Gd^{3+} in CaF_2 ,⁷ cannot be applied to the study of Gd^{3+} in ThO_2 and CeO_2 because optical data for Gd^{3+} in these lattices do not exist. However, it is interesting to note that the values of $C_{3g}^{(2)}$ and $C_{5g}^{(2)}$ are notably different for Gd^{3+} in ThO_2 and CeO_2 ; this fact is surprising in view of the similarity between these isomorphous lattices (the lattice parameter is $a = 5.411 \text{ \AA}$ for CeO_2 and 5.600 \AA for ThO_2).

We discuss briefly the temperature dependence of the second-order coefficients. Contributions arising from the thermal expansion of the crystal

TABLE I. Values of the second- and fourth-order spin-lattice coefficients related to stress of Gd^{3+} in ThO_2 and CeO_2 measured at 290°K (units in cm/dyn).

	$10^{14}C_{3g}^{(2)}$	$10^{14}C_{5g}^{(2)}$	$10^{16}C_{lg}^{(4)}$	$10^{16}C_{3g}^{(4)}$	$10^{16}C_{5g}^{(4)}$
ThO_2	-1.11 ± 0.06	-6.35 ± 0.10	0.70 ± 0.05	-1.2 ± 0.2	5.0 ± 0.7
CeO_2	-8.7 ± 0.2	1.0 ± 0.2	0.80 ± 0.07	-1.0 ± 0.3	6.5 ± 0.7

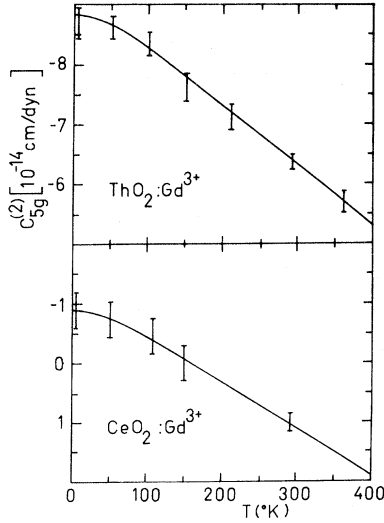


FIG. 4. Temperature dependence of the second-order trigonal spin-lattice coefficient $C_{5g}^{(2)}$ of Gd^{3+} in ThO_2 and CeO_2 . The solid line is obtained by a least-squares fit of Eq. (6) with the experimental data.

cannot explain the observed large changes of the coefficients.

Unfortunately, there are no data on the temperature variation of the elastic constants of ThO_2 and CeO_2 and we cannot estimate the contribution of this effect to the spin-lattice coefficients. However, in view of the data existing for other cubic crystals and the observed variation with temperature of the Young modulus of ThO_2 ,¹⁶ it should not account for more than 5% of the changes of the coefficients. There will be some contribution only for $C_{3g}^{(2)}$ measured in the CeO_2 crystal; in this case about one-third of the measured temperature dependence could be justified by the changes of the elastic constants with temperature, and if this contribution is subtracted, the slope of the curve would be the same as that for $C_{3g}^{(2)}$ of Gd^{3+} in ThO_2 .

We conclude then that the temperature variation of the second-order spin-lattice coefficients reported in this work is mainly due to the coupling of the ions with the lattice vibrations.

The temperature variation of a parameter C due to the coupling of the ion with the crystal vibrations through the orbit-lattice interaction could be written as

TABLE II. Values of the second- and fourth-order spin-lattice coefficients related to strain of Gd^{3+} in ThO_2 measured at 290°K. (Units in cm^{-1} .)

$G_{3g}^{(2)} = (-2.9 \pm 0.2) \times 10^{-2}$	$G_{5g}^{(2)} = (-5.1 \pm 0.1) \times 10^{-2}$
$G_{1g}^{(4)} = (4.1 \pm 0.3) \times 10^{-4}$	$G_{3g}^{(4)} = (-3.1 \pm 0.6) \times 10^{-4}$ $G_{5g}^{(4)} = (4.0 \pm 0.6) \times 10^{-4}$

TABLE III. Values of the constants $C_{3g}^{(2)}$ (RL), $C_{5g}^{(2)}$ (RL), $K_{3g}^{(2)}$, and $K_{5g}^{(2)}$ obtained by a least-squares fit of the experimental data with Eq. (6) for $\omega = 1 \times 10^{13}$ sec^{-1} . $C_{3g}^{(2)}$ (RL) and $C_{5g}^{(2)}$ (RL) are in units of 10^{-14} cm/dyn .

	$C_{3g}^{(2)}$ (RL)	$K_{3g}^{(2)}$	$C_{5g}^{(2)}$ (RL)	$K_{5g}^{(2)}$
ThO_2	-0.51 ± 0.02	-0.079 ± 0.003	-9.25 ± 0.10	0.38 ± 0.01
CeO_2	-7.50 ± 0.03	-0.153 ± 0.005	-1.21 ± 0.03	0.292 ± 0.005

$$C(T) = C_{RL} + C' \langle Q^2 \rangle, \quad (5)$$

where C_{RL} is the value of C for a rigid lattice, $\langle Q^2 \rangle$ is the thermal average over different normal modes of the square of the vibration amplitude, and C' depends on the strength of the interaction.

Several approaches could be taken for the calculation of $\langle Q^2 \rangle$. In our case, assuming that the coupling of the ion with the lattice vibrations involves mechanisms inside the f^7 configuration, only even-symmetry modes of the cube of oxygen ligands would contribute to $\langle Q^2 \rangle$. There are factors from 15 to 9 between the masses of the metal ions Th^{4+} , Ce^{4+} , and Gd^{3+} and the oxygens, and to assume an Einstein model for the vibrations of the oxygens is a good approximation.¹⁷ Then Eq. (5) can be written as

$$C(T) = C_{RL} + K \coth(\hbar\omega/2kT), \quad (6)$$

where ω is the assumed single vibrational frequency of the oxygens and K is a numerical constant. Using a least-squares analysis we obtained a good fit of our experimental data to Eq. (6) supposing that $\omega = 1 \times 10^{13}$ sec^{-1} . This value of ω is reasonable in view of the values reported by Willis¹⁷ and Ali and Nagels.¹⁸ The values of the spin-lattice coefficients corresponding to a rigid lattice C_{RL} and the constant K which depends on its temperature variation for Gd^{3+} in ThO_2 and CeO_2 are given in Table III.

We propose a mechanism involving the spin-orbit interaction V_{SO} in second order, the orbit-lattice interaction V_{OL} modulated by the crystal vibrations in second order, together with the axial crystal-line field V_{ax} introduced by the deformation which would contribute to the observed temperature variation of the spin-lattice coefficients. If we write

$$V_{OL} = \sum_{i,\alpha} V_{i,\alpha} Q_{i,\alpha},$$

where $Q_{i,\alpha}$ are the normal modes of the crystal and $V_{i,\alpha}$ are operators acting on the wave functions of the paramagnetic ion, the mechanism could be schematically represented by

$$\sum_{i,i'} \langle {}^8S_{7/2} | V_{SO} | {}^6\Gamma_4 \rangle \langle {}^6\Gamma_4 | V_{i,\alpha} | {}^6\Gamma_r \rangle \langle {}^6\Gamma_r | V_{ax} | {}^6\Gamma_{r'} \rangle \times \langle {}^6\Gamma_{r'} | V_{i',\alpha'} | {}^6\Gamma_4 \rangle \langle {}^6\Gamma_4 | V_{SO} | {}^8S_{7/2} \rangle Q_{i,\alpha} Q_{i',\alpha'}, \quad (7)$$

where $|^8S_{7/2}\rangle$ are the ground-state wave functions of the Gd^{3+} ion and $|^6\Gamma_\kappa\rangle$ are the excited states obtained from the spin sextuplets of the f^7 configuration which are eigenfunctions of the cubic crystalline field and transform like the Γ_κ irreducible representation of O_h . A detailed calculation of the mechanism proposed in Eq. (7) is a formidable problem, but it is easily seen that a result similar to that proposed in Eq. (5) could be derived from Eq. (7) for its vibrational part.

The thermal average at a given temperature is proportional to

$$\langle Q_{i,\alpha} Q_{i',\alpha'} \rangle = \delta_{i,i'} \delta_{\alpha,\alpha'} \langle Q_{i,\alpha}^2 \rangle$$

because of the incoherence of different normal modes of the crystal.

B. Fourth-Order Spin-Lattice Coefficients

Since no temperature variation has been observed for the fourth-order spin-lattice coefficients of Gd^{3+} in ThO_2 and CeO_2 we give only the values obtained at 290 °K in Tables I and II. The values measured at other temperatures agree within the experimental errors.

The strain coefficient related to a hydrostatic deformation $G_{1g}^{(4)}$ gives the variation of the cubic field parameter with the lattice parameter a . From Eq. (2) the following is obtained⁵:

$$G_{1g}^{(4)} = \frac{a}{3} \frac{dB_4}{da} \quad (8)$$

where B_4 is the cubic field parameter. dB_4/da has been measured by Hurren *et al.*¹⁹ for Eu^{2+} (iso-electronic with Gd^{3+}) in CaF_2 , SrF_2 , and BaF_2 by hydrostatic stress experiments. Our value of $G_{1g}^{(4)}$ for Gd^{3+} in ThO_2 has the same magnitude that was obtained from their data using Eq. (8).

It is interesting to note that the positive sign obtained for $G_{1g}^{(4)}$ indicates that the cubic field parameter B_4 decreases when the lattice parameter is

increased, as expected from a simple point-charge model for the crystalline field.

Data on the temperature dependence of B_4 for Gd^{3+} in ThO_2 have been reported by Marshall²⁰ and Abraham and Boatner.²¹ From Marshall's data we found

$$\frac{dB_4}{dT} = \frac{1}{60} \frac{db_4}{dT} = 1.26 \times 10^{-8} \text{ cm}^{-1}/^\circ\text{K} \quad (9)$$

at room temperature. The contribution from the thermal expansion to this temperature variation is

$$\left(\frac{dB_4}{dT} \right)_{TE} = 3\alpha G_{1g}^{(4)}$$

where α is the linear expansion coefficient. From our value of $G_{1g}^{(4)}$ for Gd^{3+} in ThO_2 and the value α (298 °K) = $0.843 \times 10^{-5} \text{ }^\circ\text{K}^{-1}$ given by Hoch and Momin²² it is found that

$$\left(\frac{dB_4}{dT} \right)_{TE} = 1.03 \times 10^{-8} \text{ cm}^{-1}/^\circ\text{K} \quad (10)$$

The difference between the values given in Eqs. (9) and (10) is consistent with the uncertainties involved in the estimation and it is concluded that the temperature variation of the cubic field parameter of Gd^{3+} is mainly due to the thermal expansion of the crystal. No other conclusion can be made at this moment about the values of the fourth-order spin-lattice coefficients and it remains for future theoretical work to describe the mechanisms contributing to these values.

ACKNOWLEDGMENTS

We are very much indebted to C. Fainstein and M. C. G. Passeggi for their help during the experiments and in the interpretation of the data. We are grateful to Dr. M. M. Abraham for providing the samples used in the experiments and to C. Lulich for very efficient technical assistance.

†Work supported in part by the Consejo Nacional de Investigaciones Científicas y Técnicas, República Argentina.

*Member of the Carrera del Investigador Científico, Consejo Nacional de Investigaciones Científicas y Técnicas, República Argentina.

¹B. G. Wybourne, *Phys. Rev.* **148**, 317 (1966).

²R. R. Sharma, T. P. Das, and R. Orbach, *Phys. Rev.* **149**, 257 (1966); **155**, 338 (1967); **171**, 378 (1968).

³M. M. Abraham, L. A. Boatner, C. B. Finch, E. J. Lee, and R. A. Weeks, *J. Phys. Chem. Solids* **28**, 81 (1967).

⁴E. R. Feher, *Phys. Rev.* **136**, A145 (1964).

⁵R. Calvo, R. A. Isaacson, and Z. Sroubek, *Phys. Rev.* **177**, 484 (1969).

⁶M. Blume and R. Orbach, *Phys. Rev.* **127**, 1587 (1962).

⁷R. Calvo, M. C. G. Passeggi, and M. Tovar, *Phys.*

Rev. B **4**, 2876 (1971).

⁸Preliminary data for Gd^{3+} in ThO_2 at 295 °K were reported by us [S. B. Oseroff, R. Calvo, and C. Fainstein, *Phys. Letters* **32A**, 393 (1970)].

⁹W. M. Walsh, J. Jeener, and N. Bloembergen, *Phys. Rev.* **139**, A1338 (1965).

¹⁰C. Fainstein and S. B. Oseroff, *Rev. Sci. Instr.* **42**, 547 (1971).

¹¹M. M. Abraham, E. J. Lee, and R. A. Weeks, *J. Phys. Chem. Solids* **26**, 1249 (1965).

¹²K. W. H. Stevens, *Proc. Phys. Soc. (London)* **A65**, 209 (1952).

¹³M. T. Hutchings, in *Solid State Physics*, edited by F. Seitz and D. Turnbull (Academic, New York, 1964), Vol. 16.

¹⁴The numerical coefficient which multiplies $C_{5g}^{(4)}$ in Eq. (14) of Ref. 5 should be $-\frac{1}{18}$ and not $-\frac{1}{8}$.

¹⁵P. M. Macedo, W. Capps, and J. B. Wachtman, Jr.,

J. Am. Ceram. Soc. **49**, 651 (1964).

¹⁶J. B. Wachtman, Jr., W. E. Tefft, D. G. Lam, Jr., and C. S. Apstein, Phys. Rev. **122**, 1754 (1961).

¹⁷B. T. M. Willis, Proc. Roy. Soc. (London) **274**, 122 (1963); **274**, 134 (1963).

¹⁸M. Ali and P. Nagels, Phys. Status Solidi **21**, 113 (1967).

¹⁹W. R. Hurren, H. M. Nelson, E. G. Larson, and

J. H. Gardner, Phys. Rev. **185**, 624 (1969).

²⁰S. A. Marshall, Phys. Rev. **159**, 191 (1967); and private communication.

²¹M. M. Abraham and L. A. Boatner, J. Chem. Phys. **51**, 3134 (1969).

²²M. Hoch and A. C. Momin, High Temp. High Press. **1**, 401 (1969).

⁵¹V Quadrupolar Effects in V-Transition-Metal Alloys and Solutions of O and N in V[†]

E. von Meerwall and T. J. Rowland

*Department of Metallurgy and Mining Engineering and Materials Research Laboratory,
University of Illinois, Urbana, Illinois 61801*

(Received 9 August 1971)

The ⁵¹V NMR in several V-based alloys with 3*d*, 4*d*, and 5*d* transition metals, and in dilute solid solutions of O and N in V, was used to study quadrupolar effects due to alloying. The results show these effects to be several times smaller for transition-metal (substitutional) solutes than for interstitial O and N in V. The solute dependence suggests that the field gradients around substitutional atoms arise mainly in response to local lattice distortion rather than to the shielding of the excess charge of the solute. A line-shape simulation based on an r^{-3} radial dependence of q produces good agreement with the observed absorption spectra. The all-or-nothing wipeout model, when applied to the interstitial alloys, yields wipeout numbers $n_1 = 126 \pm 7$ for N in V, and $n_1 = 194 \pm 12$ for O in V. The observed magnitude of the effective field gradients in V-based alloys is believed to result from a partial cancellation of the Sternheimer antishielding tendency by the overshielding effect of a large density of states near the Fermi level at the V atoms.

I. INTRODUCTION

Since the early work of Drain¹ it has been known that the nuclear-quadrupole interaction has a relatively small effect on the ⁵¹V NMR in vanadium metal and V-based alloy systems. The spin of ⁵¹V is $\frac{7}{2}$, and its electric-quadrupole moment is -0.05_2 b,² about one-third the value for ²⁷Al, ⁶³Cu, and ⁶⁵Cu, nontransition metals on which alloy studies have been previously made. For some alloys the decrease with solute concentration of the observable resonance intensity has been interpreted in terms of an all-or-nothing quadrupolar wipeout model³ to yield an effective first-order (satellite) wipeout number n_1 . For the ²⁷Al NMR in Al:Cu, $n_1 \approx 170$,⁴ while 3*d*-transition-metal solutes in Al, because of the presence of resonant ($l=2$) conduction-electron scattering,⁵ cause even larger wipeout: n_1 (²⁷Al) for Fe or Mn in Al is about 800.⁴ In all of these cases, the spectrum is also affected to second order in the quadrupolar interaction e^2qQ/h and is essentially unobservable at higher solute concentrations.

By contrast, the ⁵¹V NMR has been observed at all solute concentrations at least in the cubic phases, and where no magnetic interactions exist, in V-Ti,^{6,7} V-Cr,^{1,8} V-Mn,^{1,9,10} V-Fe,^{11,12} V-Co,¹ V-Ni,¹ and

also in V-Nb,¹³ V-Tc,^{7,14,15} V-Ru,¹⁶ and V-Al.¹⁷ In none of these cases does the peak-to-peak NMR intensity per V nucleus seem to be reduced more than an order of magnitude from that of pure-V metal. In the interstitial β -VH (V lattice body-centered tetragonal, $c/a \geq 1.10^{18}$), not even first-order distortion could be observed at room temperature.¹⁹ A detailed study of the effects of alloying on the NMR line shape in V-Mn has been reported by von Meerwall and Schreiber.¹⁰ Their findings, as they pertain to the quadrupolar distortions of the vanadium resonance, may be summarized as follows:

(a) There is a first-order wipeout effect of the peak-to-peak intensity, complete by about 15-at. % Mn in V ($n_1 = 36$), but there is no second-order broadening above 4 kOe at any concentration.

(b) The satellite intensity is removed symmetrically from the line center, but remains close to it. There is no discernible structure in the wings. Upward of 90% of the total expected intensity remains within ± 120 kHz of the center. The peak-to-peak width decreases slightly from pure V to 1.5-at. % Mn in V, and remains nearly constant to well above 15-at. % Mn in V.

(c) The electric field gradients remain below about 10^{24} cm⁻³ even at the V nuclei nearest to a Mn